Mapping the Electronic Structure and the Reactivity Trends for Stabilized α-Boryl Carbanions

Ricardo J. Maza,[a] Elena Fernández,*[a] and Jorge J. Carbó*[a]

Abstract: The chemistry of stabilized α-boryl carbanions shows remarkable diversity, and can enable many different synthetic routes towards efficient C—C bond formation. The electron-deficient, trivalent boron center stabilizes the carbanion facilitating its generation and tuning its reactivity. Here, the electronic structure and the reactivity trends of a large dataset of α-boryl carbanions are described. DFT-derived parameters were used to capture their electronic and steric properties, computational reactivity towards model substrates, and crystallographic analysis within the Cambridge Structural Dataset. This study maps the reactivity space by systematically varying the nature of the boryl moiety, the substituents of the carbanionic center, the number of α-boryl motifs, and the metal counterion. In general, the free carbanionic intermediates are described as borata-alkene species with C—B π interactions polarized towards the carbon. Furthermore, it was possible to classify the α-boryl alkylidene metal precursors into three classes directly related to their reactivity: 1) nucleophilic borata-alkene salts with alkali and alkaline earth metals, 2) nucleophilic η^2-(C—B) borata-alkene complexes with early transition metals, Cu and Ag, and 3) α-boryl alkyl complexes with late transition metals. This trend map aids selection of the appropriate reactive synthon depending on the reactivity sought.

Introduction

The access to primary, secondary, and tertiary alkylboronic esters, through the generation of α-boryl carbanions and subsequent electrophilic trapping, is a new and powerful synthetic tool towards efficient C—C bond formation. The generation of α-boryl carbanions can be conducted through four complementary pathways (Scheme 1), including a) deborrylation of 1,1-diboryl alkanes,[1–10] b) deprotonation of the α-hydrogen from an organoborane compound,[11–16] c) metallation of α-halo boronic esters[17] and d) transmetallation of α-borylmethide metal salts with organometallic reagents.[18] α-Boryl carbanions show a remarkable stability due to the valence deficiency of the adjacent three coordinate boron center, and they can be also described by their borata-alkene resonance forms (Scheme 2).[19,20]

The experimental outcomes are consistent with the delocalization of the electron density of the anion throughout the empty p orbital of the adjacent boron. This is demonstrated by the chemical shifts displacement on ^{11}B (highfield) and ^{13}C (downfield) NMR data for $R_2B\text{-}CH_2^-$ in comparison with the
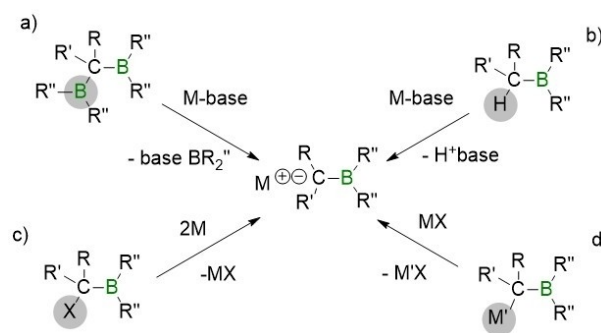
Scheme 1. Strategic methods to access α-boryl carbanions.
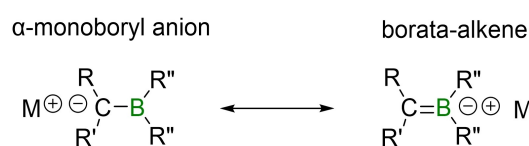
Scheme 2. Resonance structures for α-boryl carbanion and borata-alkene.

corresponding α-boryl alkane.[12,21] IR spectra of boron-stabilized anions in the gas phase, in combination with DFT calculations, also suggest the double bond character of C=B bond in $Me_2BCH_2^-$ α-monoboryl anions.[22]

In the solid state, the shortened B—C bond lengths[23-25] of the borata-alkene species provide an additional evidence of the their "boron ylide" character, which can be related to the analogs containing boron–carbon double bonds.[26] Computational studies have also supported the borata-alkene character of α-boryl carbanions by means of detailed analysis of their electronic structures.[25,27,28] The natural bond orbital (NBO)

[a] R. J. Maza, Prof. E. Fernández, Dr. J. J. Carbó
Universitat Rovira i Virgili, Departament de Química Física i Inorgànica
43007 Tarragona (Spain)
E-mail: mariaelena.fernandez@urv.cat
        j.carbo@urv.cat

Chemistry—A European Journal

Full Paper
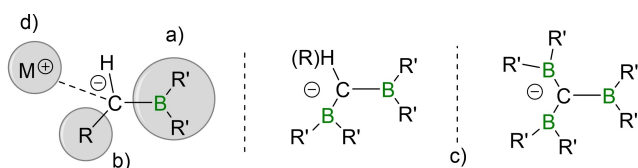doi.org/10.1002/chem.202101464

**Chemistry
Europe**

European Chemical
Societies Publishing

analysis on [Mes₂B=CR₂]⁻ anion by Gabbaï et al. showed one σ- and one π-interaction between the carbon and the boron atoms, where the π bond was polarized towards the carbon.[27] Erker et al. described a similar B—C interaction for related species, in which the HOMO formally corresponds to a C—B π-orbital strongly polarized towards the carbanionic atom.[25]

The study by Erker et al.[25] compared three different α-boryl moieties, $B(C_6F_5)_2$, $BMes_2$ and 9-boryilbicyclo[3.3.1]nonane (Scheme 3). The authors concluded that the high degree of carbanion stabilization when the boryl moiety $B(C_6F_5)_2$ is involved might be due to the presence of fluorine substituents on the aryl group. The mesityl substituents at boron led to a decrease of stabilization by about 16 kcal mol⁻¹, followed by the borata-alkenes containing the 9-boryilbicyclo[3.3.1]nonane which showed a lower degree of carbanion stabilization (Scheme 3). The steric protection of the boron center seems to be necessary to ensure an appropriate proton abstraction of the α-hydrogen from the organoborane (Scheme 1b), since there is a strong tendency to form a four-coordinate boron"ate" salt upon addition of a base. For that reason, most of the borata-alkenes reported so far bear bulky substituents on boron, such as $B(C_6F_5)_2$, $BMes_2$ or 9-boryilbicyclo[3.3.1]nonane. Eventually, the pronounced α-boryl carbanion stabilization represents an extra advantage to explore the significant reactivity of the borata-alkenes.[25,29]

To gain more insight into the electronic structure and the reactivity trends of α-boryl carbanions, we conduct here a detailed computational study based on density functional calculations (ωB97X-D functional) and wave function analysis. The study is performed on a varied dataset of compounds bearing commonly used boryl moieties, such as Bpin (pinacol-boryl) and Bdan (naphthodiazaboryl). As illustrated in Scheme 4, we have gauged the influence of several structural features of the α-boryl carbanions: a) the nature of the boryl moiety, b) the substituents on the carbanionic center, c) the comparison between α-mono-, α-di- and α-triboryl carbanions, and d) the
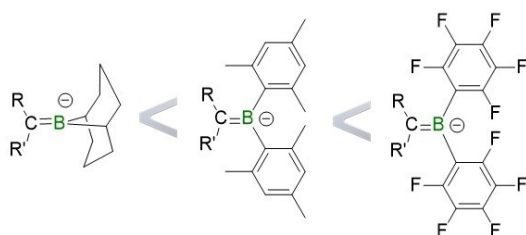
nature of the metal involved. Ultimately, we aim to identify reliable descriptors derived from ground-state structures that correlate with the stability and reactivity of α-boryl carbanions and allow to build a map of trends for these species.

Results and Discussion

Influence of the nature of the boryl moiety

Using as starting point, the early work by Erker et al.,[25] we have initially gauged the electronic structure and reactivity of α-monoboryl carbanions as a function of boryl fragment nature. We started with the comparison of the previously analyzed α-monoboryl carbanions, containing the boryl moieties $BMes_2$ and $B(C_6F_5)_2$ (**1a^mes** and **1a^PhF**), with those that include the commonly used Bpin and Bdan moieties in the structure, (**1a^pin** and **1a^dan** respectively). Here, we have explored different geometric, electronic and energy descriptors aiming to rationalize the stability and reactivity trends along the carbanion series. Table 1 collects the values of the most meaningful descriptors for **1a^PhF**, **1a^mes**, **1a^dan** and **1a^pin** species; and Tables S1 and S2 in the Supporting Information lists all the computed descriptors and their values.

In line with the analysis reported by Erker et al.,[25] the stabilization of α-boryl carbanions can be assessed by calculating the protonation energies of the carbanions with respect to the cyclopentadienyl anion (ΔG_{prot}) as illustrated in Scheme 5. Note that this calculation is equivalent to compute absolute proton affinities of carbanions but using cyclopenatadienyl as reference to set the zero, that is, subtracting the proton affinity of cyclopentadienyl (368.4 kcal mol⁻¹) to each species. More-

Scheme 3. Stabilizing order for selected borata-alkene species.

Scheme 4. Analyzed structural features influencing the nature of the α-boryl carbanions.

Table 1. Calculated protonation Gibbs energies (ΔG_{prot} [kcal mol⁻¹]) and free-energy barriers for nucleophilic substitution with bromoethane ($\Delta G^{\ddagger}_{S_N2}$ [kcal mol⁻¹]), energy of the HOMO orbital (E_{HOMO} [eV]), and Wiberg bond orders upon variation of boryl moiety nature ($\Sigma C-B_{bo}$), species **1a^PhF**, **1a^mes**, **1a^dan** and **1a^pin**.

	1a^PhF	1a^mes	1a^dan	1a^pin
$\Delta G_{prot.}$	+19.7	−0.2	−23.2	−33.6
$\Delta G^{\ddagger}_{S_N2}$	19.3	18.8	6.9	4.2
$\Sigma C-B_{bo}$	1.73	1.69	1.57	1.56
E_{HOMO}	−2.87	−2.20	−1.19	−0.58

Scheme 5. Protonation of α-boryl carbanion with cyclopentadiene.

Chemistry–A European Journal

Full Paper
doi.org/10.1002/chem.202101464

**Chemistry
Europe**
European Chemical
Societies Publishing

over, we have determined the free-energy barriers ($\Delta G^{\pm}_{S_N2}$) for the S_N2 nucleophilic substitution reaction between the carbanions and bromoethane (Scheme 6) in order to quantify the nucleophilic reactivity of α-boryl carbanions towards organic electrophiles. The values of energy barriers in Table 1 indicate the following trend on the reactivity $1a^{pin} > 1a^{dan} > 1a^{mes} > 1a^{PhF}$.

The reactivity trend is inversely correlated to the stability of the α-monoboryl carbanions. The least reactive species $1a^{mes}$ and $1a^{PhF}$ show a marked stabilization as reflected in isoenergetic or endergonic, relative protonation free-energies ($\Delta G_{prot} = -0.2$ and $+19.7$ kcal mol^{-1}, respectively). Whereas the boron atom in $1a^{PhF}$ and $1a^{mes}$ is protected by the steric bulkiness of Mes and C$_6$F$_5$ groups, the Bpin and Bdan boryl fragments depict the π-donor ability from the O and N heteroatoms to the empty p orbital of the B atom. Consequently, in $1a^{mes}$ and $1a^{PhF}$ the electron deficient boron center is fully available for delocalizing the carbanion negative charge. This also correlates with the Wiberg C—B bond order whose values increase from $1a^{pin} < 1a^{dan} < 1a^{mes} < 1a^{PhF}$ (Table 1). Moreover, the values are significantly larger than 1 (from 1.56 to 1.73), supporting the borata-alkene character of these species.

The nucleophilic reactivity of organic reagents has been traditionally correlated with the energy level of HOMO orbital, or with the NBO atomic charges as we reported for related nucleophilic boryl species.[30,31] Here, the energy of the HOMO, formally corresponding to a C—B π-orbital strongly polarized towards the carbanionic atom (Figure 1), clearly correlates with the nucleophilic reactivity. The higher the energy is, the lower the free energy barrier (compare 2nd and 4th files in Table 1).

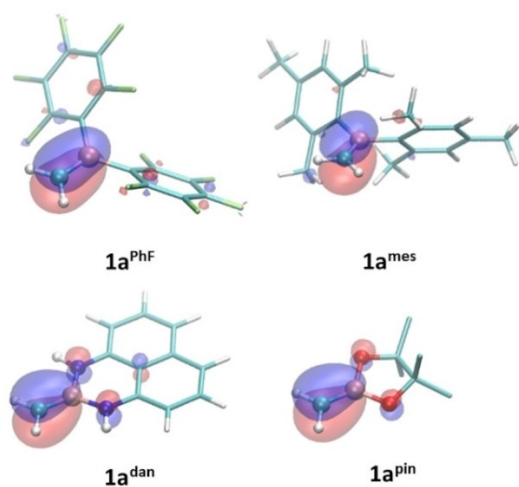**Scheme 6.** Alkylation of α-boryl carbanion with bromoethane.

Figure 1. Representation of HOMO orbitals, formally corresponding to a C—B π-orbital polarized towards the carbon, for $1a^{PhF}$, $1a^{mes}$, $1a^{dan}$ and $1a^{pin}$.

Interestingly, the $1a^{pin}$ species is computed to be more reactive than $1a^{dan}$ ($\Delta G^{\pm}_{S_N2} = 4.2$ and 6.9 kcal mol^{-1}, respectively).

As illustrated in the HOMO representations of Figure 1, the aromatic fragment of Bdan $1a^{dan}$ moiety contributes to the delocalization of the carbanionic charge through the π-channel, resulting in lower energy-laying HOMO compared to $1a^{pin}$. In fact, we had observed this effect in a previous study on boron-stabilized carbanions generated from deborylation of 1,1-diborylalkanes with alkoxides.[32] As the N atoms bound to B in Bdan are better π-donors than O atoms in Bpin, one can envisage that in the absence of the aromatic fragment, the diazoboryl moieties should enhance carbanion nucleophilicity. To evaluate this effect, we computed the unprecedented compound $1a^{Npin}$ (Scheme 7), in which the O substituents on $1a^{pin}$ were replaced by NH fragments. In line with previous reasoning, the $1a^{Npin}$ is the most reactive species with a computed free energy barrier $\Delta G^{\pm}_{S_N2}$ of only 3.2 kcal mol^{-1}. Finally, it is worth to mention that in this subset, the computed atomic charges at the carbanionic carbon (-0.88, -0.98, -1.14 and -1.20 a.u. for $1a^{PhF}$, $1a^{mes}$, $1a^{dan}$ and $1a^{pin}$, respectively) are consistent with the nucleophilicity of the α-boryl methyl fragment, but this correlation is not observed for the other subsets in this work. A similar trend was suggested by Erker et al.[25] who attributed the observation to their borata-alkane behavior. Therefore, HOMO energies will be used hereafter as a suitable descriptor of the reactivity of α-boryl carbanions.
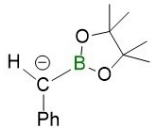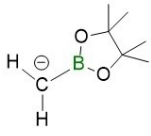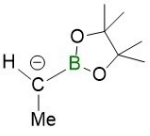
Influence of the substituents on the carbanionic carbon

We explored next how the reactivity/stability and electronic structural properties can be affected by the influence of Me and Ph substituents on α-monoboryl carbanions. The calculated ΔG_{prot} energies for $1c^{pin}$ (Table 2) demonstrates that the Ph group stabilizes the carbanion lone pair. This is also reflected in a larger sum of Wiberg bond orders for the three bonds of carbanion (3.68 for $1c^{pin}$ vs. 3.55 and 3.62 for $1a^{pin}$ and $1b^{pin}$, respectively), and in the lower energy-laying HOMO (-1.27 for $1c^{pin}$ vs. -0.58 and -0.56 eV for $1a^{pin}$ and $1b^{pin}$, respectively). Both descriptors capture the electron withdrawing effect of the Ph group. In line with the trend in stability, $1c^{pin}$ shows lower reactivity for the S_N2 nucleophilic substitution of bromoethane than for $1a^{pin}$ ($\Delta G^{\pm}_{S_N2} = 9.8$ and 4.2 kcal mol^{-1} for $1c^{pin}$ and $1a^{pin}$, respectively).

The presence of the Me group ($1b^{pin}$) does not alter significantly the nucleophilic character of the carbanion respect to hydrogen-substituted $1a^{pin}$. Although it is usually considered
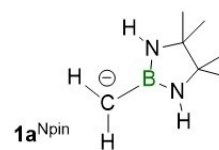
Scheme 7. Schematic representation of the newly designed 4,4,5,5-tetramethyl-1,3,2-diazaboryl methide anion $1a^{Npin}$.

12354

Chemistry–A European Journal

Full Paper
doi.org/10.1002/chem.202101464

Chemistry Europe
European Chemical
Societies Publishing

Table 2. Calculated protonation Gibbs energies ($\Delta G_{prot.}$ [kcal mol^{-1}]), free-energy barriers for nucleophilic substitution in bromoethane ($\Delta G_{S_N2}^{\ddagger}$ [kcal mol^{-1}]) in, energy of the HOMO (E_{HOMO} [eV]), and Wiberg bond orders upon variation of carbanion substituents, species **1c^{pin}**, **1a^{pin}** and **1b^{pin}**.

Species	1c^{pin}	1a^{pin}	1b^{pin}
$\Delta G_{prot.}$	−7.2	−33.6	−30.6
$\Delta G_{S_N2}^{\ddagger}$ [a]	9.8 (13.0)	4.2 (9.3)	4.2 (8.5)
ΣC–R$_3$ bond order [b]	3.68	3.55	3.62
E_{HOMO}	−1.27	−0.58	−0.56

[a] Values in parenthesis correspond to calculations with continuum solvent mode (DMSO). [b] Sum of Wiberg bond orders for the three bonds of carbanion (C–B, C–H, and C–Ph/–H/–Me).

Table 3. Calculated protonation Gibbs energies ($\Delta G_{prot.}$ [kcal mol^{-1}]) and free-energy barriers for nucleophilic substitution in bromoethane ($\Delta G_{S_N2}^{\ddagger}$ [kcal mol^{-1}]), energy of the HOMO orbital (E_{HOMO} [eV]), Wiberg bond orders, and average C–B distances in Å upon variation of the number of boryl substituens, species **1a^{pin}**, **2a^{2pin}** and **3^{3pin}**.

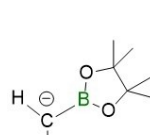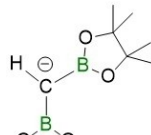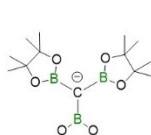| Species	1a^{pin}	2a^{2pin}	3^{3pin}
$\Delta G_{prot.}$	−33.6	−10.0	−1.8
$\Delta G_{S_N2}^{\ddagger}$	4.2	10.3	14.0
ΣC–R$_3$ bond order	3.55	3.51	3.39
C–B$_{bo-av.}$	1.56	1.23	1.07
d_{C-B} av.	1.44	1.47	1.50
E_{HOMO}	−0.58	−1.85	−2.61

that alkyl groups destabilize carbanions due to their electron-donating inductive effect, here calculations show that other subtle effects need to be considered since they do not provide a clear picture of stability/reactivity order between **1a^{pin}** and **1b^{pin}** (Table 2). Besides the inductive effect one should considerer an electrostatic size effect, in which the negative charge in **1b^{pin}** is more stabilized by the larger molecular volume that reduces its charge density. Thus, calculations in vacuum pointed out that methyl-substituted **1b^{pin}** is more stable (less negative ΔG_{prot}) than **1a^{pin}**, whereas its HOMO is higher in energy (−0.58 and −0.56 eV for **1a^{pin}** and **1b^{pin}**, respectively). However, inclusion of the effect of polar solvent reduces the influence of electrostatic size effect, and the corresponding calculations predict that methyl-substituted **1b^{pin}** is more reactive than **1a^{pin}** (see values in parenthesis in Table 2).

Influence of the number of boryl substituents

We next explored the influence of the number of boryl fragments in the stability/reactivity of the corresponding carbanions. Table 3 compares the main computed parameters for α-mono-, di-, and triboryl carbanions **1a^{pin}**, **2a^{2pin}** and **3^{3pin}**, respectively. Increasing the number of boryl moieties the stability of the carbanion is enhanced (**1a^{pin}** < **2a^{2pin}** < **3^{3pin}**) whereas the nucleophilicity is reduced (**1a^{pin}** > **2a^{2pin}** > **3^{3pin}**). Figure 2 shows the HOMO orbitals for **2a^{2pin}** and **3^{3pin}**, where it can be clearly observed that each boryl moiety contributes to the stabilization of the carbanion through a strong delocalization of the carbanion p-type electron density into the π channel. Consequently, the α-triboryl carbanion **3^{3pin}** has lower-energy laying HOMO (−2.61 eV) than those for **2a^{2pin}** and **1a^{pin}** (−1.85 and −0.58 eV, respectively) being the former the least prone to react with electrophiles and the most stable.

Remarkably, the sums of Wiberg bond order of the carbanion for species **1a^{pin}**, **2a^{2pin}** and **3^{3pin}** (3.55, 3.51 and 3.39, respectively) do not seem to be consistent with their stability. In this case, the most stable **3^{3pin}** species has the lowest overall
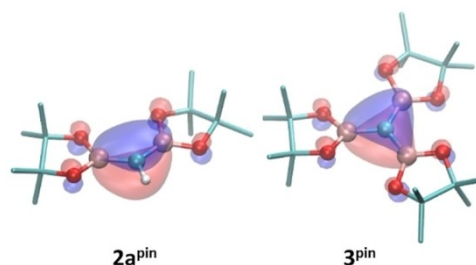
Figure 2. Representation of HOMO orbitals, formally corresponding to a C–B π-orbital polarized towards the carbon, for **2a^{2pin}** and **3^{3pin}**.

bond order. This might be due to the loss of borata-alkane character when the negative charge of carbanion has to be shared between several boryl moieties. In fact, the averaged individual C–B bond order in **3^{3pin}** is low (1.07) and the averaged C–B bond distance (1.50 Å) is significantly longer than that for monoborylated species **1a^{pin}** (1.44 Å). Thus, multi-boryl carbanions can be viewed as carbanionic species with polar C–B bonds, in which the excess of negative charge is electrostatically stabilized by the boron substituents, as well as, by some amount of charge transfer to the empty perpendicular boron p orbitals. Figure 3 depicts the evolution of computed atomic
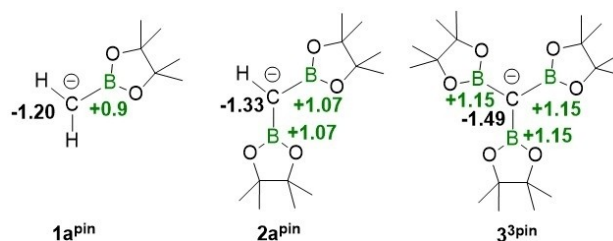
Figure 3. NBO atomic charges for mono-, di-, and triboryl carbanions **1a^{pin}** (Δq_{B-C} = 2.10), **2a^{2pin}** (Δq_{B-C} = 2.40), and **3^{3pin}** (Δq_{B-C} = 2.64).

Chemistry–A European Journal

Full Paper
doi.org/10.1002/chem.202101464

Chemistry
Europe
European Chemical
Societies Publishing

charges from mono- to di-, and to tri-boryl carbanions, showing an increasing charge separation (polarization) at the C—B bonds. The estimated amount of charge transferred from the carbanion to the perpendicular boron p orbitals is still significant for **3³ᵖⁱⁿ** (0.21 a.u.), contributing to the overall stabilization of this species (Table S3).

Mapping the nucleophilicity of α-boryl carbanions

Once it has been discussed in detail the influence of electronic and structural features on the stability/reactivity of several model α-boryl carbanions, our next objective is the construction of a map from a full set of structures, in order to classify and identify certain trends in the chemical space. To this end, we additionally analyzed 14 α-boryl carbanions depicted in Figure 4. Overall, the full dataset (**set 1**) comprises 22 anionic species, which were selected by varying systematically the number and the type of boryl moieties, as well as, the type of substituents on carbon (R = H, Me and Ph). The dataset also includes the α-boryl vinyl system (**1eᵖⁱⁿ**), in order to compare the borata-alkene character between $[R_2B=CH_2]^-$ and $[R_2B=CH=CH_2]^-$. Interestingly, we found an inverse, linear correlation (correlation coefficient $r^2 = 0.91$) between the protonation energies of the carbanions and the HOMO energies, which can be consequently used as reliable descriptor to gauge the stability/reactivity trends in α-boryl carbanions (Figure S1).

Figure 5 maps the full dataset using two descriptors, the energy of the HOMO (E_{HOMO}) and the sum of Wiberg C—B bond order (ΣC—B$_{bo}$). The E_{HOMO} descriptor can be directly related to the stability/reactivity trends, while the ΣC—B$_{bo}$ is a useful descriptor allowing to separate the mono-, di- and triborylated species, and to differentiate between Me and Ph substituents on carbon. First, we identified a clear correlation between the number of boryl substituents and the carbanion nucleophilicity as reflected in the HOMO energy. α-Triboryl carbanions are the least nucleophilic, with HOMO energies ranging from −3.3 to −2.6 eV, presumably due to the accumulation of the three stabilizing boryl substituents. The reactivity on these species follows the trend **3³ᵖⁱⁿ** > **3²ᵖⁱⁿᵈᵃⁿ** > **3ᵖⁱⁿ²ᵈᵃⁿ** > **3³ᵈᵃⁿ** in agreement with the observation that Bdan moieties have an extra stabilization effect on the carbanion.[32] Within the α-diboryl carbanions, the calculated HOMO energies are found between −2.6 to −1.7 eV, conforming a specific group where once again the species containing Bdan units become less reactive and more stabilized than the ones with Bpin moieties. In fact, the

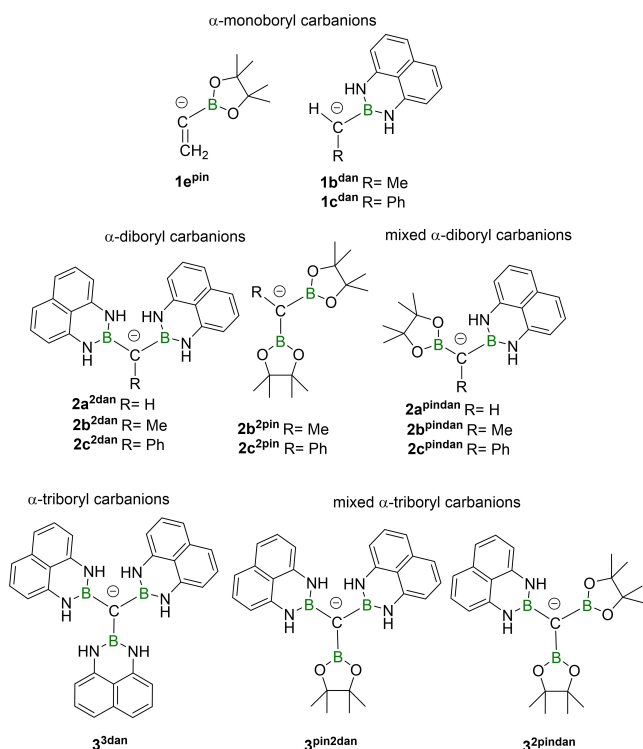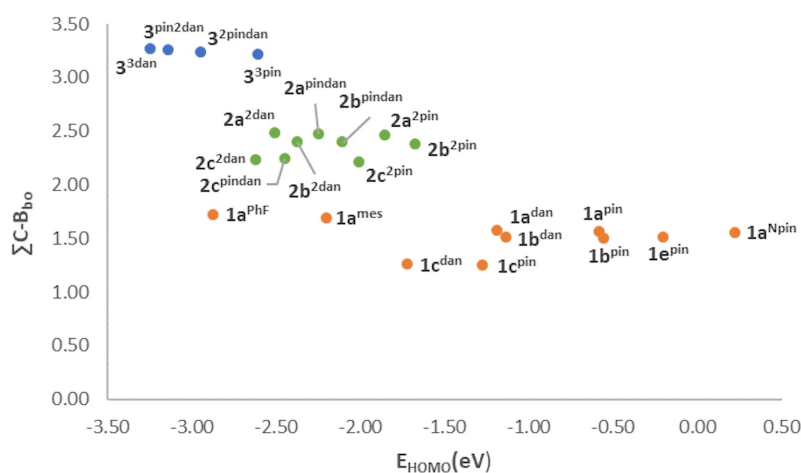**Figure 4.** Additional α-boryl carbanion species forming dataset **set1**.

Figure 5. Representation of the sum of C—B Wiberg bond orders versus the energy of the HOMO [eV] for α-monoboryl (•), α-diboryl (•), and α-triboryl (•) carbanions.

Chemistry–A European Journal

Full Paper
doi.org/10.1002/chem.202101464

**Chemistry
Europe**
European Chemical
Societies Publishing

values for HOMO energy for **2a**[2dan] and **2c**[2dan] carbanions reach values close to the next group to the left, the α-triboryl carbanions (Figure 5). The mixed α-diboryl cabanions (**2a**[pindan], **2b**[pindan], and **2c**[pindan]) have intermediate energy HOMO values, and the **2b**[2pin] might be the most reactive among the α-diboryl carbanions.

The subset formed by the α-monoborylated species with Bpin or Bdan boryl fragments shows higher HOMO energies (−1.3 to −0.2 eV). Among them, we predicted the vinyl carbanionic species **1e**[pin], that contains a sp² carbanion, as highly nucleophilic. Even more to the right, we found the newly designed species **1a**[Npin] (Scheme 7). Whereas the sum of Wiberg C—B bond order for **1a**[Npin] is similar to **1a**[pin], the higher energy of the HOMO orbital of **1a**[Npin] indicates that combining N-substituted boron and non-aromatic scaffold causes the largest nucleophilicity. On the other side, the species containing highly acidic BMes or BC₆H₅ moieties (**1a**[mes] and **1a**[PhF]) have E_{HOMO} values that lay in the range of di- and triborylated species (−2.2 and −2.9 eV, respectively). This clearly indicates that boryl substituents in **1a**[mes] and **1a**[PhF] cause a strong stabilization on the carbanion because in the absence of heteroatom substituents on boron, its perpendicular p orbital is fully available for the overlap with the lone pair of the carbanion.

The structures with the phenyl substituents (**1c**[pin], **1c**[dan], **2c**[2pin], **2c**[pindan] and **2c**[2dan]) show the lowest C—B bond orders due to the electron-releasing effect of the phenyl groups, which compete with electron delocalization through the borata-alkene structure. On the other hand, the structures containing methyl substituents (**1b**[pin], **1b**[dan], **2b**[2pin], **2b**[pindan] and **2b**[2dan]) have slightly lower C—B bond orders than those species with hydrogen substituents. This latter trend can be correlated with a subtle effect of alkyl substituents, which induce some electrostatic delocalization.

Influence of the nature of the metal

The practical applications of borata-alkenes as reactive synthons are achieved by different strategies which involve the preparation of boryl alkylidene metal salts and α-boryl alkyl transition metal complexes. Here, we study the influence of those metals and transition metals in their stability/reactivity. Figure 6 depicts the selected structures including Li⁺, Cu⁺, Ag⁺ and Pd²⁺ α-boryl methide metal salts, and Table 4 collects the most representative computed parameters. In this case, to evaluate the nucleophilic reactivity, we have determined the free-energy barriers ($\Delta G^{\ddagger}_{Ald}$) required to transfer the carbanions to the electrophilic carbon atom of the model substrate formaldehyde (Scheme 8). This substrate is a simple species that have been used to quantify the reactivity of related metal-boryl compounds,[31,33] and constitute a model of observed reactions such as the nucleophilic borylmethylation of aldehydes with α-boryl alkyl copper[34] and silver[35] complexes, and with lithium dimesithylboron substituted carbanions [(Mes)₂BC(H)RLi].[36] It is important to note that for Li, Cu and Ag species the nucleophilic additions to several organic electrophiles have been reported,[34–37] while for transition metals such as Pd the
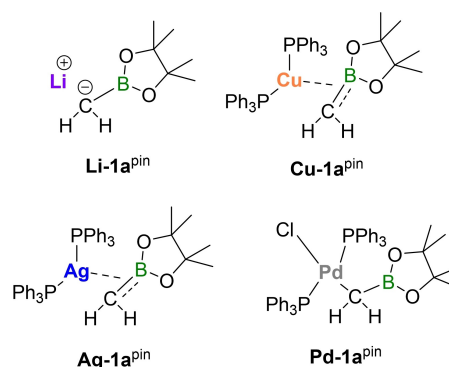

Figure 6. Selected structures for the analysis of the effect of the metal cation (Li⁺, Cu⁺, Ag⁺, and Pd²⁺) on the stability/reactivity of α-boryl carbanionic species.

Table 4. Calculated free-energy barriers for carbanion addition to formaldehyde ($\Delta G^{\ddagger}_{Ald}$ [kcal mol⁻¹]), overall charge of carbanion fragment ($q[C]$), Wiberg bond orders, C—B lengths (d_{C-B} [Å]), and steric distance–weight volume (V_W) upon variation the cationic fragment in **1a**[pin]-**Li**, **1a**[pin]-**Cu**, **1a**[pin]-**Ag** and **1a**[pin]-**Pd**.

Structure	1a[pin]-Li	1a[pin]-Cu	1a[pin]-Ag	1a[pin]-Pd
$\Delta G^{\ddagger}_{Ald}$ [a]	2.2ª	15.0	18.4	52.7
$q[C]$	−0.88	−0.66	−0.64	−0.21
C—B bond order	1.36	1.17	1.17	0.97
d_{C-B}	1.48	1.51	1.51	1.55
V_W	0.0	40.6	38.1	46.3

[a] The free-energy barrier is computed from a precursor complex in which the carbonyl oxygen of aldehyde is coordinated side-on to lithium.
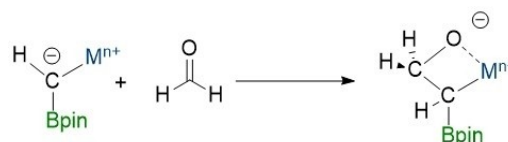
Scheme 8. Nucleophilic addition of α-boryl methide metals to formaldehyde.

observed reactivity involves mainly transmetalation processes.[38] Thus, we should expect low to moderate free-energy barriers for Li, Cu and Ag salts, and larger barrier for Pd indicating a less favorable nucleophilic reactivity.

The computed $\Delta G^{\ddagger}_{Ald}$ values (Table 4) predict an order of nucleophilic reactivity that is consistent with experimental background (Li > Cu > Ag > Pd, with $\Delta G^{\ddagger}_{Ald} = 2.2$, 15.0, 18.4, and 52.7 kcal mol⁻¹, respectively). Here, we identify the overall charge of carbanionic fragment ($q[C]$) as descriptor correlating with nucleophilicity; thus, the more negatively charged the carbanionic fragment, the lower is the energy barrier (Table 4, second row). The formation of coordination complexes changes the nature of the HOMO orbital which cannot be univocally assigned to the C—B π-interaction, and consequently, we discarded it as descriptor in this case. Additionally, we evaluated the steric effects of the different metal fragments on the reactivity using the distance-weighted volume (V_W)

Chemistry–A European Journal

Full Paper
doi.org/10.1002/chem.202101464

Chemistry Europe
European Chemical
Societies Publishing

parameter.[39,40] The V_W parameter measures the steric bulkiness of the metal fragment and its impact on carbanion center (see Computational Methods). Comparison of the closely related [(PPh$_3$)$_2$Cu(H$_2$CBpin)] and [(PPh$_3$)$_2$Ag(H$_2$CBpin)] complexes shows that the silver fragment induces less steric hindrance on the reactive carbanion due to the larger size of Ag$^+$ ion, which move away the ligand substituents. However, the larger polarization of the metal-carbon bond in Cu complex determines its higher nucleophilicity, indicating that steric effects are less influential than electronic ones when comparing different metals.

Along the series we observe substantial structural changes in the boron-carbon moiety and in its interaction with the metal (Table 4, third and fourth rows). This indicates a continuous switch on the compound nature from borata-alkene lithium salt to a α-boryl alkyl palladium complex. In lithium species **1a^{pin}-Li**, both the Wiberg C—B bond order (1.36) and the C—B distance (1.48 Å) are indicative of borata-alkene character. The Li cation interacts electrostatically with the three atoms of O—C—B moiety (Figure 7). Although Li$^+$ does not change the nature of the species, it induces some C—B lengthening (+0.04 Å) and pyramidalization of the carbanionic carbon (−30°), with respect to the free carbanion **1a^{pin}**. Note that introducing specific solvation molecules solvating Li$^+$ cation[41] would diminish its effect on the electronic structure of borata-alkene. On the other extreme, the computed C—B bond order of palladium complex **1a^{pin}-Pd** is close to 1 and the corresponding distance (1.55 Å) is significantly larger than for **1a^{pin}-Li**. Thus, this Pd compound can be better defined as an α-boryl alkyl palladium complex. At an intermediate situation, the Bpin=CH$_2$$^-$ fragment in Cu and Ag compounds acts as an anionic η^2-(C,B) ligand whose interaction with the transition metal is shifted toward the C atom (Figure 7). In line with bonding description, the HOMO orbital in **1a^{pin}-Cu** and **1a^{pin}-Ag** shows an overlap between transition metal d orbitals and the C=B π orbital (Figure S4). Note that borata-alkenes acting as anionic ligands with η^2 coordination to transition metals are known.[42]
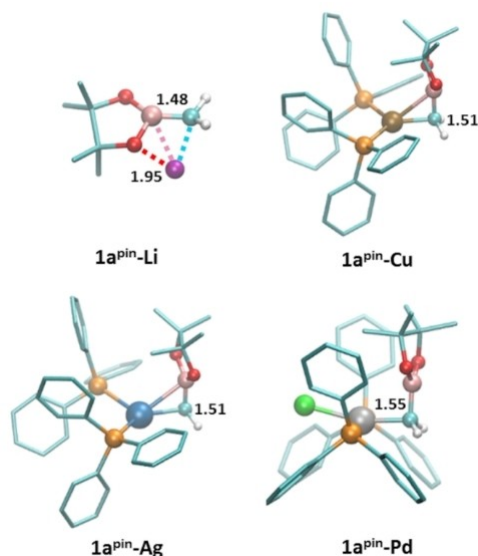

Figure 7. Three-dimensional representation of computed structures for metal complexes **1a^{pin}-Li, 1a^{pin}-Cu, 1a^{pin}-Ag** and **1a^{pin}-Pd**. Selected bond lengths are given in Å.

Trend map for metal salts and complexes

To further assess the variation in the nature of α-boryl carbanions with regard to the metal involved, we performed a systematic structural search within the Cambridge Structural Database (CSD; see Computational Methods), and constructed a histogram of the C=B bond lengths (Figure 8). The graph separates the crystallographic data for boryl methide salts into three main groups: red bars represents boryl methide Li salts, green bars covers boryl methide Cu salts, and other metals from group 4 and 5, and blue bars involve boryl methide salts of late transition metals including Pd^{2+}. For each group, the d(C—B) values lie within a relatively wide range (0.1 Å), but their distributions are centered at different distances. To the far left we found the boryl alkylidene lithium salts, most of whose C—B distances range from 1.44 to 1.49 Å. Moving to the right, from 1.47 to 1.54 Å, there are several early transition metal complexes (Ti^{4+}, Zr^{4+}, Hf^{4+}, and Ta^{5+}), and within this distance range

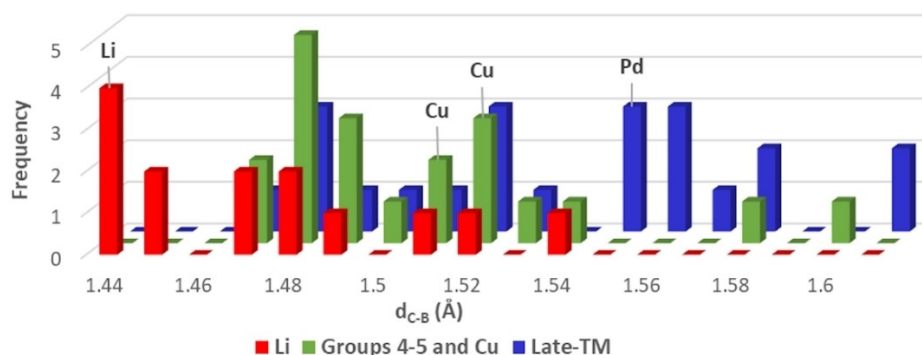**Figure 8.** Histograms for B—C bond lengths of α-boryl carbanionic species separated into 3 groups as a function of carbanion nature: 1) Li salts (•), 2) Cu and groups 4 and 5 including Ti, Zr, Hf, and Ta complexes (•), and 3) late transition metals including Fe, Ru, Rh, Ni, Pd, Pt, Au, Zn and Hg (•). All bonds lengths are rounded to the nearest 0.01 Å. Data obtained from crystallographic data in the CSD.

Chemistry–A European Journal

Full Paper
doi.org/10.1002/chem.202101464

**Chemistry
Europe**
European Chemical
Societies Publishing

we also found the Cu^+ complexes at 1.51 and 1.52 Å. At longer C—B distances (>1.52 Å), we find most of the late transition metal complexes such as Pd, Pt, Ru, Rh or Zn (see Table S4 for a complete list). Overall, our computed values fit quite well with the structural data available in CSD, allowing to classify the nature of α-boryl carbanionic species into three main groups and to establish structure-reactivity relationships.

The borata-alkene lithium salts, and the η^2-(C,B) borata-alkene copper and silver complexes show highly polarized metal-carbon interactions with a significant nucleophilic character. They are prone to generate carbanionic fragments stabilized by boryl moiety that are able to react with organic electrophiles as observed experimentally.[34–37] Other promising species for nucleophilic additions are those based on early transition metals, although to the best of our knowledge their reactivity has not been tested yet.[37] Only few examples are currently reported on the use of silver salts for nucleophilic additions.[35] The α-boryl alkyl palladium complexes have less polarized and stronger metal-carbon bond. As consequence, the reported reactivity for Pd differs from Li, Cu and Ag. Although these palladium complexes do not serve as nucleophilic agents, they have been applied in C—C bond forming reactions, for example, by transmetalation.[38] Figure 8 shows that other late transition metals have similar structural features to Pd, suggesting that this reactivity can be extended to other complexes.

Finally, Figure 9 provides an extension of the electronic structure analysis for Li, Cu, Ag and Pd compounds with different type and number of boryl moieties and substituents on the carbanionic atom. The overall charge of the carbanionic fragment ($q[C]$) and the average C—B bond order (C—$B_{bo\text{-}av.}$) can be used as descriptors to evaluate the nucleophilicity and the nature of the α-boryl carbanionic species, respectively. Clearly, the extent of the nucleophilicity (increasing to the left of the graph) is mainly ruled by the type of metal, but it can be tuned by α-boryl carbanionic fragment. We also observe that the decrease of C—B bond order, that is, the reduction of borata-

alkene character, has the following trend: Li $>$ Cu $\cong$ Ag $>$ Pd. The C—$B_{bo\text{-}av.}$ descriptor is more sensitive to the nature of the carbanionic fragment. Interestingly, among Cu species, calculations suggest that the vinyl carbanionic **1e**^{pin}-Cu complex is located at a different area of the chemical space (Figure 9), and therefore, it could lead to new reactivity.

Conclusion

We have systematically studied several types of α-boryl carbanion, analyzing their electronic structures and reactivity trends as a function of the nature of boryl moieties, the type of carbanionic substituents, the number of boryl motifs, and the metal interaction with the carbanion. In general, the free carbanionic intermediates are better described as borata-alkene species with a C—B π-interaction strongly polarized towards the carbanionic atom. By taking into consideration the energy of the HOMO and Wiberg bond order, we were able to establish a gradient of stability and nucleophilic reactivity for these intermediates. π-Acidic boron atoms (i.e., $BMes_2$ or $B(C_5F_5)_2$), aromatic substituents on boron (i.e., Bdan), or electron withdrawing substituents on carbon (i.e., Ph) induce a larger delocalization of the carbanionic charge through the π-channel that results in more stable and less reactive intermediates. The multi-boryl carbanionic species lose part of their borata-alkene character but enhance their stability electrostatically through the additive effect of several polar C—B bonds. This map of the reactivity landscape has predicted a novel α-boryl carbanion, the newly designed 4,4,5,5-tetramethyl-1,3,2-diazaboryl methide anion **1a**^{Npin} $[H_2CB(NH)_2R_2]^-$, which should show enhanced nucleophilicity.

For α-boryl alkylidene metal precursors, both computational and crystallographic analysis of a large dataset identify three different types of carbanionic species that can be directly related to the observed reactivity: 1) borata-alkene salts with
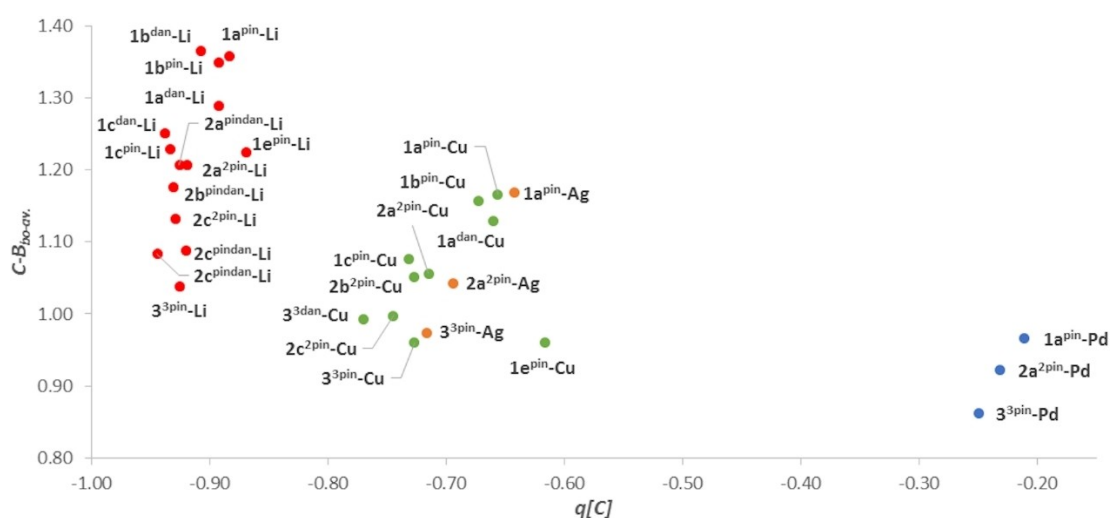

Figure 9. Representation of the average of C—B Wiberg bond orders (C—$B_{bo\text{-}av.}$) versus the overall charge of the carbanionic fragment ($q[C]$) for the α-boryl carbanionic Li (•), Cu (•), Ag (•) and Pd (•) species.

Chemistry–A European Journal

Full Paper
doi.org/10.1002/chem.202101464

Chemistry Europe
European Chemical
Societies Publishing

alkali and alkaline earth metals such as Li, 2) η^2-(C–B) borata-alkene complexes with early transition metals, Cu and Ag, and 3) α-boryl alkyl complexes with late transition metals such as Pd. The two first groups show highly polarized metal-carbon interactions with a significant nucleophilic character that make them suitable synthons for reacting with organic electrophiles. The third group has a less polarized and stronger metal-carbon bond, and they are prone to undergoing other types of C–C bond forming reactions such as cross coupling through trans-metalation strategies. We hope that this map and the under-lying dataset will facilitate the optimization of novel α-boryl carbanion reagents and assist their selection along with the desired reactivity parameters, contributing to the developing of this emerging area in chemistry.

Computational Methods

Geometry optimizations and transition state searches were per-formed with Gaussian16[43] package. The quantum mechanics calculations were performed within the framework of density functional theory (DFT)[44] by using the ωB97X–D functional.[45] The basis set employed effective core potentials (ECPs) with double-ζ valence basis set (LANDL2DZ)[46] for Cu, Ag, Pd, Cl, Br and P, and were supplemented with polarized shells with the following exponents: Cu ($f = 3.525$), Ag ($f = 1.611$), Pd ($f = 1.472$), Cl ($d = 0.650$), Br ($d = 0.428$) and P ($d = 0.387$).[47] For all other electrons of all other atoms 6–31G(d) basis set was used.[48] The solvent effects of DMSO were included by means of SMD model[49] as implemented in Gaussian16.[43] The bonding of the molecules as well as the fragment charges were analyzed by using the NBO method,[50] from which we derived the Wiberg bond order and carbanion fragment charge ($q[C]$) descriptors. The NBO method analyses the resultant wave function in terms of optimally chosen localized orbitals, corresponding to a Lewis structure representation of chemical bonding. For computing orbital populations consistently, we had defined the carbanion carbon bonded to 3 substituents with single bonds.

To quantify the steric hindrance of metal fragments, we used the distance-weighed volume parameter (V_W).[39,40] which measures the steric bulkiness of the molecular environment and its impact on the carbanion center. The descriptor quantifies the bulk produced the metal fragment by considering three parameters: 1) The number of atoms, excluding the metal, 2) the size of the atom ($r =$ van der Waals radii [Å]), and 3) the distance (d [Å]) from the atom to the boron center. The factor r^3 is divided by d for each atom, and the sum is extended to all of the atoms in the given fragment. Finally, the crystallographic structure search was carried out by using CSD software, using the February 2020 version. A data set collection of computational results is available in the ioChem-BD repository and can be accessed at https://doi.org/10.19061/iochem-bd-2-52.[51]

Acknowledgements

Conflict of Interest

The authors declare no conflict of interest.

[1] G. Cainelli, G. Dal Bello, G. Zubiani, *Tetrahedron Lett.* **1965**, *6*, 3429–3432.
[2] G. Zweifel, R. B. Steele, *Tetrahedron Lett.* **1966**, *48*, 6021–6025.
[3] L. Homer, H. Hoffmann, H. G. Wippel, *Chem. Ber.* **1958**, *91*, 61–63.
[4] H. Schmidbauer, W. Tronich, *Chem. Ber.* **1968**, *101*, 3556–3561.
[5] T. Kauffmann, R. Joussen, N. Klas, A. Vahrenhorst, *Top. Curr. Sci.* **1980**, *92*, 109–147.
[6] T. Kauffmann, *Angew. Chem. Int. Ed.* **1982**, *21*, 410–429; *Angew. Chem.* **1982**, *94*, 401–420.
[7] T. Kauffmann, R. Joussen, N. Klas, A. Vahrenhorst, *Tetrahedron Lett.* **1978**, *19*, 4391–4395.
[8] F. Bertini, P. Grasselli, G. Zubiani, G. Cainelli, *Tetrahedron* **1970**, *26*, 1281–1290.
[9] G. Zweifel, R. P. Fisher, A. Horng, *Synthesis* **1972**, 557–558.
[10] G. Zweifel, H. Arzoumanian, *J. Am. Chem. Soc.* **1967**, *89*, 291–295.
[11] a) M. W. Rathke, R. Kow, *J. Am. Chem. Soc.* **1972**, *94*, 6854–6856; b) R. Kow, M. Rathke, *J. Am. Chem. Soc.* **1973**, *95*, 2715–2716.
[12] A. J. Ashe III, P. Shu, *J. Am. Chem. Soc.* **1971**, *93*, 1804–1805.
[13] A. Pelter, B. Singaram, L. Warren, J. W. Win *Tetrahedron* **1993**, *49*, 2965–2978.
[14] A. Pelter, B. Singaram, L. Williams, J. W. Wilson, *Tetrahedron Lett.* **1983**, *24*, 623–626.
[15] A. Pelter, L. Williams, J. W. Wilson, *Tetrahedron Lett.* **1983**, *24*, 627–630.
[16] A. Pelter, B. Singaram, J. W. Wilson, *Tetrahedron Lett.* **1983**, *24*, 631–634.
[17] P. Knochel, *J. Am. Chem. Soc.* **1990**, *112*, 7431–7333.
[18] a) D. S. Matteson, J. W. Wilson, *Organometallics* **1985**, *4*, 1690–1694; b) D. J. S. Tsai, D. S. Matteson, *Organometallics* **1983**, *2*, 236–241.
[19] a) H. C. Brown, G. Zweifel, *J. Am. Chem. Soc.* **1961**, *83*, 3834–3840; b) G. Zweifel, H. Arzoumanian, *Tetrahedron Lett.* **1966**, *7*, 2535–2538; c) D. S. Matteson, *Synthesis* **1975**, 147–158; d) P. Paetzold, B. Boeke, *Chem. Ber.* **1976**, *109*, 1011–1016.
[20] R. J. Maza, J. J. Carbó, E. Fernández, *Adv. Synth. Catal.* **2021**, *363*, 2274–2289.
[21] K. Hong, X. Liu, J. P. Morken, *J. Am. Chem. Soc.* **2014**, *136*, 10581–10584.
[22] J. Oomens, J. D. Steill, Th. H. Morton, *Inorg. Chem.* **2010**, *49*, 6781–6783.
[23] R. A. Bartlett, P. P. Power, *Organometallics* **1986**, *5*, 1916–1917.
[24] M. M. Olmstead, P. P. Power, K. J. Weese, R. J. Doedens, *J. Am. Chem. Soc.* **1987**, *109*, 2541–2542.
[25] P. Moquist, G.-Q. Chen, Ch. Mück-Lichtenfeld, K. Bussmann, C. G. Daniliuc, G. Kehr, G. Erker, *Chem. Sci.* **2015**, *6*, 816–825.
[26] P. P. Power, *Chem. Rev.* **1999**, *99*, 3463–3504.
[27] Ch.-W. Chiu, F. P. Gabbaï, *Angew. Chem. Int. Ed.* **2007**, *46*, 6878–6881; *Angew. Chem.* **2007**, *119*, 7002–7005.
[28] M. Lafage, A. Pujol, N. Saffon-Merceron, N. Mezailles, *ACS Catal.* **2016**, *6*, 3030–3035.
[29] T. Klis, S. Lulinski, J. Serwatowski, *Curr. Org. Chem.* **2010**, *14*, 2549–2566.
[30] J. Cid, J. J. Carbó, E. Fernández, *Chem. Eur. J.* **2012**, *18*, 12794–12802.
[31] D. García-López, J. Cid, R. Marqués, E. Fernández, J. J. Carbó, *Chem. Eur. J.* **2017**, *23*, 5066–5075.
[32] A. B. Cuenca, J. Cid, D. García-López, J. J. Carbó, E. Fernández, *Org. Biomol. Chem.* **2015**, *13*, 9659–9664.
[33] a) M. Wagner, N. J. R. van Eikema Hommes, H. Nöth, P. v. R. Schleyer, *Inorg. Chem.* **1995**, *34*, 607–614; b) H. Zhao, L. Dang, T. b. Marder, Z. Lin, *J. Am. Chem. Soc.* **2008**, *130*, 5586–5594.
[34] a) M. V. Joannou, B. S. Moyer, S. J. Meek, *J. Am. Chem. Soc.* **2015**, *137*, 6176–6179; b) S. A. Murray, J. C. Green, S. B. Tailor, S. J. Meek, *Angew. Chem. Int. Ed.* **2016**, *55*, 9065–9069; *Angew. Chem.* **2016**, *128*, 9211–9215.
[35] M. V. Joannou, B. S. Moyer, M. J. Goldfogel, S. J. Meek, *Angew. Chem. Int. Ed.* **2015**, *54*, 14141–14145; *Angew. Chem.* **2015**, *127*, 14347–14351.
[36] A. Pelter, D. Buss, E. Colclough, B. Singaram, *Tetrahedron* **1993**, *49*, 7077–7103.
[37] For some reviews reporting additional examples of nucleophilic additions of Li and Cu boryl stabilized carbanions, see: a) N. Miralles, R. J. Maza, E. Fernández, *Adv. Synth. Catal.* **2018**, *360*, 1306–1327; b) Ch.

Wu, J. B. Wang, *Tetrahedron Lett.* **2018**, *59*, 2128–2140; c) R. Nallagonda, K. Padala, A. Masarwa, *Org. Biomol. Chem.* **2018**, *16*, 1050–1064.

[38] a) Ch. Zhang, X. Wu, Ch. Wang, Ch. Zhang, J. Qu, Y. Chen, *Org. Lett.* **2020**, *16*, 6376–6381; b) Ch. Li, M. Li, J. Li, W. Wu, H. Jiang, *Chem. Commun.* **2018**, *54*, 66–69.

[39] a) S. Aguado-Ullate, S. Saureu, L. Guasch, J. J. Carbó, *Chem. Eur. J.* **2012**, *18*, 995–1005; b) S. Aguado-Ullate, M. Urbano, I. Villaba, E. Pires, J. I. García, C. Bo, J. J. Carbó, *Chem. Eur. J.* **2012**, *18*, 14026–14036.

[40] *MolQuO application* (accessed May 2021): http://rodi.urv.es/~carbo/quadrants/index.html

[41] J. Royes, S. Ni, A. Farré, E. La–Cascia, J. J. Carbó, A. B. Cuenca, F. Maseras, E. Ferández, *ACS Catal.* **2018**, *8*, 2833–2838.

[42] For a review, see: D. J. H. Emslie, B. E. Cowie, K. B. Kolpin, *Dalton Trans.* **2012**, *41*, 1101–1117.

[43] Gaussian 16, Revision A.03, M. J. Frisch, G. W. Trucks, H. B. Schlegel, G. E. Scuseria, M. A. Robb, J. R. Cheeseman, G. Scalmani, V. Barone, G. A. Petersson, H. Nakatsuji, X. Li, M. Caricato, A. V. Marenich, J. Bloino, B. G. Janesko, R. Gomperts, B. Mennucci, H. P. Hratchian, J. V. Ortiz, A. F. Izmaylov, J. L. Sonnenberg, D. Williams-Young, F. Ding, F. Lipparini, F. Egidi, J. Goings, B. Peng, A. Petrone, T. Henderson, D. Ranasinghe, V. G. Zakrzewski, Gao, N. Rega, G. Zheng, W. Liang, M. Hada, M. Ehara, K. Toyota, R. Fukuda, J. Hasegawa, M. Ishida, T. Nakajima, Y. Honda, O. Kitao, H. Nakai, T. Vreven, K. Throssell, J. A., Jr. Montgomery, J. E. Peralta, F. Ogliaro, M. J. Bearpark, J. J. Heyd, E. N. Brothers, K. N. Kudin, V. N. Staroverov, T. A. Keith, R. Kobayashi, J. Normand, K. Raghavachari, A. P. Rendell, J. C. Burant, S. S. Iyengar, J. Tomasi, M. Cossi, J. M. Millam, M. Klene, C. Adamo, R. Cammi, J. W. Ochterski, R. L. Martin, K. Morokuma, O. Farkas, J. B. Foresman, D. J. Fox, Gaussian, Inc., Wallingford CT, **2016**.

[44] R. G. Parr, W. Yang, *Density Functional Theory of Atoms and Molecules*, Oxford University Press, Oxford, **1989**.

[45] J. D. Chai, M. Head-Gordon, *Phys. Chem. Chem. Phys.* **2008**, *10*, 6615–6620.

[46] a) P. J. Hay, W. R. Wadt, *J. Chem. Phys.* **1985**, *82*, 270–283; b) P. J. Hay, W. R. Wadt, *J. Chem. Phys.* **1985**, *82*, 284–298; c) P. J. Hay, W. R. Wadt, *J. Chem. Phys.* **1985**, *82*, 299–310.

[47] a) A. Höllwarth, M. Böhme, S. Dapprich, A. W. Ehlers, A. Gobbi, V. Jonas, K. F. Köler, R. Stegmann, A. Veldkamp, G. Frenking, *Chem. Phys. Lett.* **1993**, *208*, 237–240; b) A. W. Ehlers, M. Böhme, S. Dapprich, A. Gobbi, A. Höllwarth, V. Jonas, K. F. Köhler, R. Stegmann, A. Veldkamp, G. Frenking, *Chem. Phys. Lett.* **1993**, *208*, 111–114.

[48] a) M. S. Gordon, *Chem. Phys. Lett.* **1980**, *76*, 163–168; b) R. C. J. Binning, L. A. Curtiss, *J. Comput. Chem.* **1990**, *11*, 1206–1216; c) K. Fukui, *J. Phys. Chem.* **1970**, *74*, 4161–4163.

[49] A. V. Marenich, C. J. Cramer, D. G. J. Truhlar, *Phys. Chem. B* **2009**, *113*, 6378–6396.

[50] A. E. Reed, L. A. Curtiss, F. Weinhold, *Chem. Rev.* **1988**, *88*, 899–926.

[51] M. Álvarez-Moreno, C. de Graaf, N. Lopez, F. Maseras, J. M. Poblet, C. Bo, *J. Chem. Inf. Model.* **2015**, *55*, 95–103.